ADVANCED HEALTHCARE MATERIALS
www.advhealthmat.de

In Situ Insonation of Alkaline Buffer Containing Liposomes Leads to a Net Improvement of the Therapeutic Outcome in a Triple Negative Breast Cancer Murine Model

Deyssy Patrucco, Juan Carlos Cutrin, Dario Livio Longo, Elena Botto, Li Cong, Silvio Aime, and Daniela Delli Castelli*

Breast cancer is characterized by an acidic micro-environment. Acidic extracellular pH gives cancer cells an evolutionary advantage, hence, neutralization of the extracellular pH has been considered as a potential therapeutic strategy. To address the issue of systemic pH alteration, an approach based on the targeted delivery of the buffering solution to the tumor region is investigated. The method relies on the use of low frequency ultrasound and sono-sensitive liposomes loaded with buffers at alkaline pH (LipHUS). After the i.v. injection of LipHUS, the application of ultrasound (US) at the sites of the pathology induces a local increase of pH that results highly effective in i) inhibiting primary tumor growth, ii) reducing tumor recurrence after surgery, and iii) suppressing metastases' formation. The experiments are carried out on a triple negative breast cancer mouse model. The results obtained demonstrate that localized and triggered release of bicarbonate or PBS buffer from sonosensitive liposomes represents an efficient therapeutic tool for treating triple-negative breast cancer. This approach holds promise for potential clinical translation.

1. Introduction

Despite significant advances in therapy, breast cancer still ranks as the 5th leading cause of cancer-related deaths.[1] In particular, triple-negative breast cancer (TNBC) is an aggressive subtype of breast cancer characterized by the absence on cell membrane of estrogen receptor (ER), progesterone receptor (PR), and human epidermal growth factor receptor 2 (HER2) receptor. Due to its high invasiveness, metastatic potential, and lack of therapeutic targets, TNBC exhibits a high rate of early recurrence. Patients typically experience relapse within 5 years after surgery, leading to a very poor overall prognosis.[2–4] This situation claims for a continuous attention for finding improved therapeutic treatments. Recent years have witnessed a growing interest toward pH deregulation phenomena taking place both in the intracellular and extracellular tumor microenvironment. Such metabolic reprogramming involves intracellular alkalinization of cancer cells and an extracellular micro-environmental acidosis.[5–10]

The poor perfusion and the high metabolic rates are responsible for generating hypoxic and acidic regions within solid tumors. In tumor cells, the enhanced glucose catabolism yields a marked increase of lactate and H^+ that are transported outside the cell (leaving the intracellular pH at normal or even alkaline values). Aerobic glycolysis generates large amounts of CO_2 (formed by oxidation in the tricarboxylic acid cycle) that, once escaped into the extracellular space, are hydrated by extracellular membrane-bound carbonic anhydrases to yield bicarbonate and H^+. In the extracellular space, in the presence of a limited buffering capacity and reduced vascular drain, the environment becomes acidic.[11] Moreover, as tumor cells are known to prefer anaerobic glycolysis even in normoxic condition (Warburg effect) the consequent increase of glucose consumption further contributes to decrease the extracellular pH. The pH deregulation confers to cancer cells and tissues important advantages, such as the enhancement of their resistance to hypoxia and cancer therapy.[12,13] In particular, the presence of an acidic tumor environment plays a significant role in tumor progression and it is often associated to increased invasion and metastases' formation as well as resistance to drug therapy[14] and immune suppression,[15] making chemotherapy less efficient and rising the risk of relapse.

D. Patrucco, J. C. Cutrin, D. Delli Castelli
Department of Molecular Biotechnology and Health Science
University of Turin
Via Nizza 52, Turin 10126, Italy
D. L. Longo, E. Botto
Istituto di Biostrutture e Bioimmagini (IBB)
Consiglio Nazionale delle Ricerche (CNR)
Via Tommaso De Amicis, 95, Naples 80145, Italy
L. Cong
Key Laboratory of Smart Drug Delivery
Ministry of Education
School of Pharmacy
Fudan University
Shanghai 201203, China
S. Aime
IRCCS SDN
SYNLAB
Via Gianturco 113, Naples 80143, Italy
E-mail: silvio.aime@unito.it

The ORCID identification number(s) for the author(s) of this article can be found under https://doi.org/10.1002/adhm.202301480

DOI: 10.1002/adhm.202301480

On this basis, much attention has been devoted to modify the extracellular pH, either directly or indirectly.[16–19] One of the most straightforward approaches that have been used to increase the extracellular tumor pH consists of the oral administration of sodium bicarbonate and lysine buffer.[20,21] This treatment proved to be very promising both for its ability to affect the primary tumor growth and for its efficiency to impact on of the metastatic process.[22,23] However, attempts to translate this process into the clinic failed due to the poor tolerance of the patients to the systemic treatment.

In this work we report the results of our study aimed at avoiding the side effects associated to the systemic administration of the alkalinization buffer. We chose to exploit sonosensitive liposomes loaded with bicarbonate or phosphate basic buffers and to induce a local release limited, as much as possible, to the tumor region or to areas involved in the metastases' formation process. Sonosensitive liposomes have been successfully used to selectively deliver drugs to the region of interest.[24,25] In the present study, the used liposomes (LipHUS) will release the alkaline buffer payload to increase the local pH upon the application of suitable US stimuli. The nanocarriers have to be highly stable in order to maintain the pH gradient between intra and extracellular compartment until the US activation is applied.[26]

A wide variety of biomedical imaging techniques (e.g., fluorescence imaging, PET, and MRI) have been investigated in the last twenty years to measure pH in vivo not invasively.[27] Among the pH mapping MRI techniques, MRI-CEST with Iopamidol showed to be a robust tool to assess tumor acidosis and to monitor pH modifications upon therapeutic treatments, providing images endowed with high spatial resolution.[28] Hence it was decided to apply this method to monitor the efficacy of the in situ release.

2. Results

Sonosensitive liposomes are phospholipidic vesicles whose membranes can be temporarily permeabilized, upon the action of ultrasound stimuli, to release their intraliposomal payload. The membrane composition of the sonosensitive liposomes used in this work is as follows: DPPC/DSPC/Chol/DSPE-PEG-2000-methoxy in the respective molar ratio of 10:5:4:1. To be able to increase the environmental pH, a solution containing bicarbonate buffer, 150 mM at pH 10.0 (LipHUS HCO_3^-) or phosphate buffer 100 mM at pH 8 (LipHUS HPO_4^{2-}) was entrapped in the inner compartment

2.1. In Vitro Characterization of the Sonosensitive Liposomes Loaded with an Alkaline Payload

Liposomes were prepared using the thin film method and extruded in order to obtain nanoparticles with a mean diameter of 145 nm (±5.41) (**Figure 1**B). The swelling solution was composed of HCO_3^- 150 mM at pH 10. The nanoparticle size distribution polydispersity index (PDI) of 0.052 (±0.02) was assessed by dynamic light scattering (Figure 1B). An exhaustive dialysis in NaCl 0.15 M allowed to obtain a suspension of nanovesicles with an external pH (pH_e) of 7.2 (±0.13) and internal pH (pH_i) of 10.0 (Figure 1A). This pH gradient is the peculiarity of these LipHosomes[26] and it is expected that the pH gradient is maintained until when the payload is released upon the application of the US. To evaluate the pH gradient stability, the liposomes' suspensions were kept at 25 or 55 °C for 15 min under continuous pH monitoring. The thermal release is an established method for promoting the massive release of the liposome's payload. The temperature at which it occurs depends on the composition of the phospholipids of the membrane that define the transition temperature (T_c) for a given liposome. At the T_c, lipids undergo a transition ("melting") from a gel to liquid phase causing the release of the payload. The transition temperature for the herein used membrane composition is 55 °C. At room temperature the pH of the liposomal suspension remained stable whereas the heated suspension displayed a marked increase of pH, reaching the final value of 9.1 (±0.2). These results clearly indicate that the intraliposomal bicarbonate solution was released and the pH gradient removed. When the experiments were repeated by suspending the liposomal solution in PBS buffer, the lipHosomes resulted stable at room temperature with no pH variations whereas at 55 °C the expected payload release took place but the PBS medium buffered the pH change, yielding a final value close to 7.5 (±0.04).

The pH gradient stability was further investigated in conditions mimicking the in vivo conditions. The stability of LipHosomes was monitored over 3 h at 37 °C by measuring the pH of the liposomes' suspension in i) NaCl isotonic solution (solution A); ii) in PBS (solution B); iii) in human serum (HS) reconstituted in NaCl (solution C); iv) in HS reconstituted in PBS (solution D) (**Figure 2**).

The pH of the specimen A was stable for the first hour with a slight increase after 2 h, remaining close to the neutrality values (7.2–7.4). In the case of the specimen B, the pH was stable for at least 2 h (7.2–7.4). These findings indicate that the lipHosomes are quite stable and, also in the case there is some release of the basic payload, the solution is able to buffer the amount of released sodium bicarbonate.

When the LipHosomes were suspended in human serum reconstituted in NaCl (Specimen C) the solution pH remained stable only for the first 15 min; after one hour it exceeded the physiological pH and 2 h later it reached a value of 7.8. This means that in human serum, lipHosomes are less stable and the pH gradient is difficult to be maintained after 1 h. The main players in the destabilization of the liposomal membrane in human serum are represented by lipoproteins able of interfering with the packaging of the phospholipid bilayer.

For specimen D, where the lipHosomes were suspended in human serum rehydrated in PBS buffer (physiological conditions), the pH resulted stable for the first 15 min, then started to increase slowly remaining within the maximum value of the physiological range (pH of 7.4). Likely the release of bicarbonate is the same as for solution C but the presence of PBS prevents the pH to rise above 7.4. Being specimen D the one that better mimics the physiological conditions encountered by lipHUS when injected into the blood stream, we draw the conclusion that no systemic alkalinization is expected to occur after the in vivo administration of LipHosomes in the slot of time elapsing between the injection and the US insonation step.

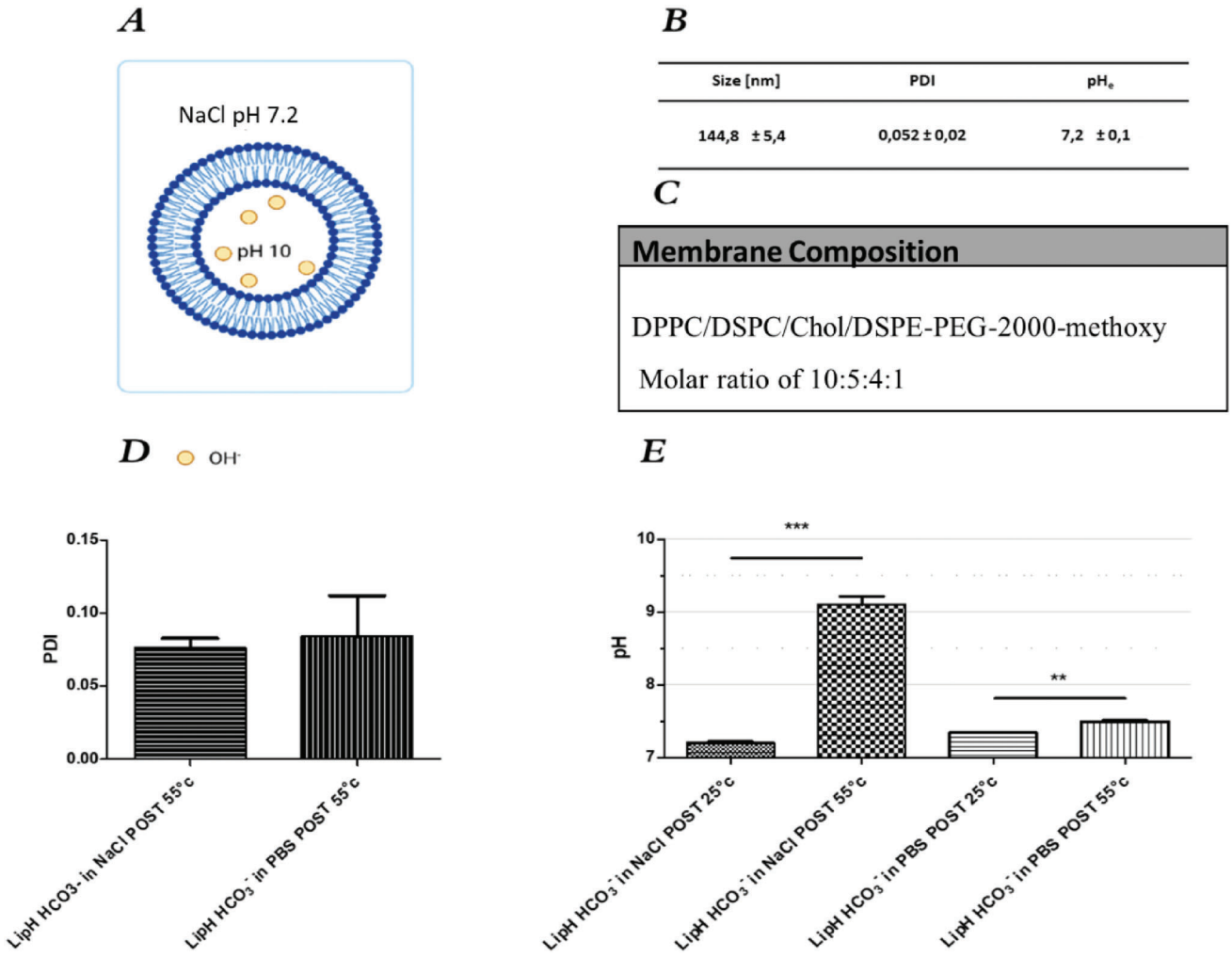

Figure 1. Characterization of HCO_3^- loaded LipHosome. A) Schematic picture of the lipHosome with indication of the pH values for the intra and extra liposomal compartments. B) Liposome dimensions measured by means of dynamic light scattering. C) Membrane phospholipidic composition. D) Effect of thermal treatment on the PDI value relative to the LipHosomes size distribution. E) pH values of the HCO_3^- loaded LipHosomes suspensions in NaCl or PBS kept at 25 °C or 55 °C.

The in vitro study of HPO_4^{2-} loading lipHosomes showed an almost identical behavior in terms of the overall stability and the release response to US stimuli. The details of these experiments are reported in the Supporting Information (Figure S1, Supporting Information).

2.2. In Vitro Tests to Assess the Liposomal Payload Release upon US Stimuli

The lipHosomes of specimen A were subjected to low intensity pulsed ultrasound waves at different acoustic pressure, varying the amplitude in the wave generator. The obtained results suggest that it is possible to control the release of the payloads from these nanosystems by applying an increasing acoustic pressure. Upon rising the amplitude to 300 mVpp, an increase in the solution pH from 7.2 to 9.3 ± 0.2 was measured (**Figure 3**B). Indeed there is a linear relationship between the amplitude and the measured pH (R^2 0.954) in the range of US amplitude from 255 to 300 mVpp (Figure 3A). Above 300 mVpp bicarbonate is fully released. These results indicate that one may control the bicarbonate dose released from the nanosystem by acting on the ultrasound-generating device. Interestingly the measured PDI after the application of the US stimuli is very similar to the one measured pre-stimuli (p-value 0.5), suggesting that the release of the payload does not significantly affect the size of the nanovesicles (Figure 3C). Upon the application of acoustic waves on lipHosomes of specimen A, a marked enhancement of the solution pH was observed (p-value < 0.0001), whereas the same treatment on lipHosomes of the specimen B resulted only in a slight pH increase, in analogy to what observed above in the case of the thermally activated release (Figure 2D).

2.3. Effect of the LipHUS Treatment on Primary Tumor Growth

To get an in-depth assessment of the LipHUS treatment on the primary tumor growth it was necessary to design a set of

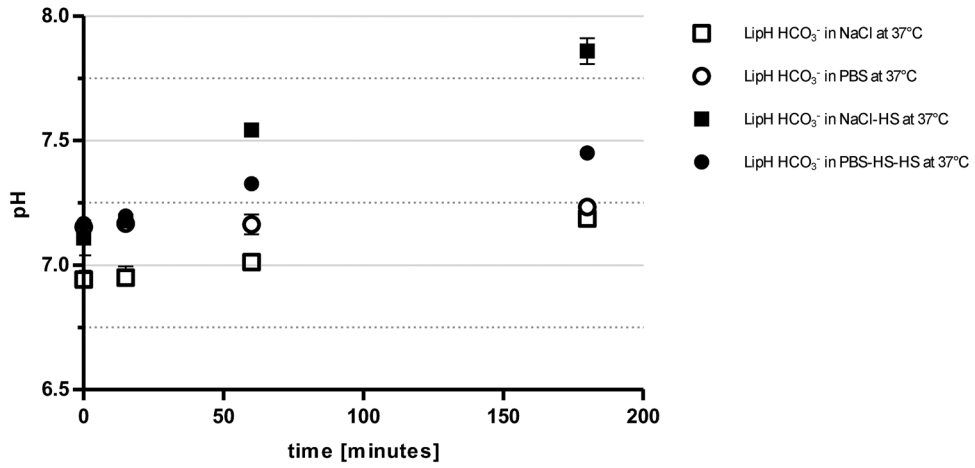

Figure 2. Measurement of solution pH variations of HCO_3^- loading LipHosomes at 37 °C. A) LipHosomes suspended in NaCl 0.15 M at pH 6.9 (white square), B) LipHosomes suspended in PBS buffer at pH 7.1 (white circle), C) LipHosomes suspended in Human Serum reconstituted in NaCl (black square), D) LipHosomes suspended in human serum reconstituted in PBS (black circle); similar results were obtained when the LipHosomes were suspended in murine serum (Figure S2, Supporting Information).

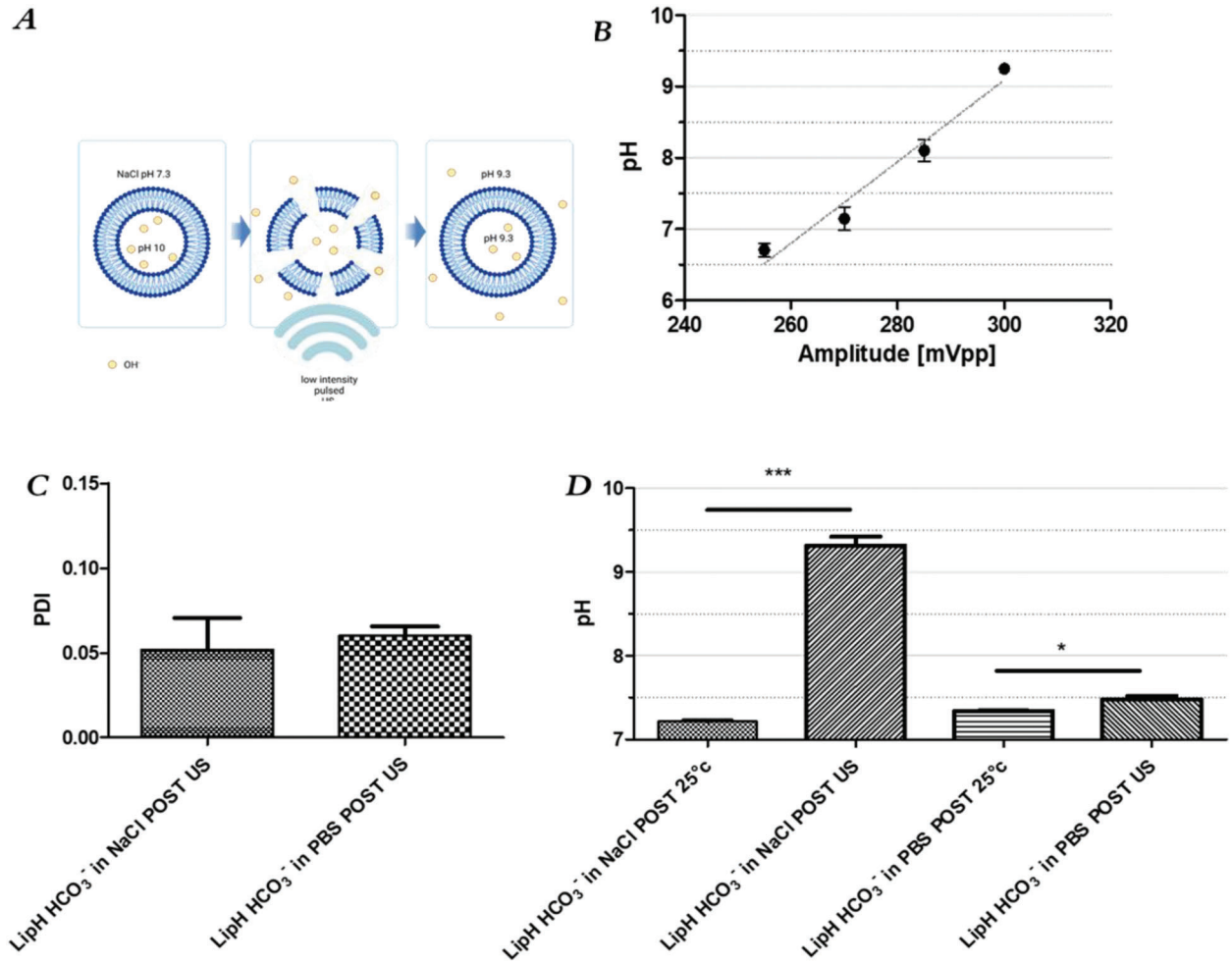

Figure 3. In vitro tests to assess the payload release from LipHosomes upon the application of US stimuli. A) Sketch to represent the effect of ultrasound stimuli to induce the payload release from lipHosomes. B) Solution pH values measured after the application of the US at different amplitude to the LipHosomes suspension (specimen A). C) Measured PDI values for the LipHosomes' suspension (specimens A and B) after the application of US. D) Solution pH measured for LipH HCO_3^- suspensions (specimens A and B) pre- and post the application of US stimuli.

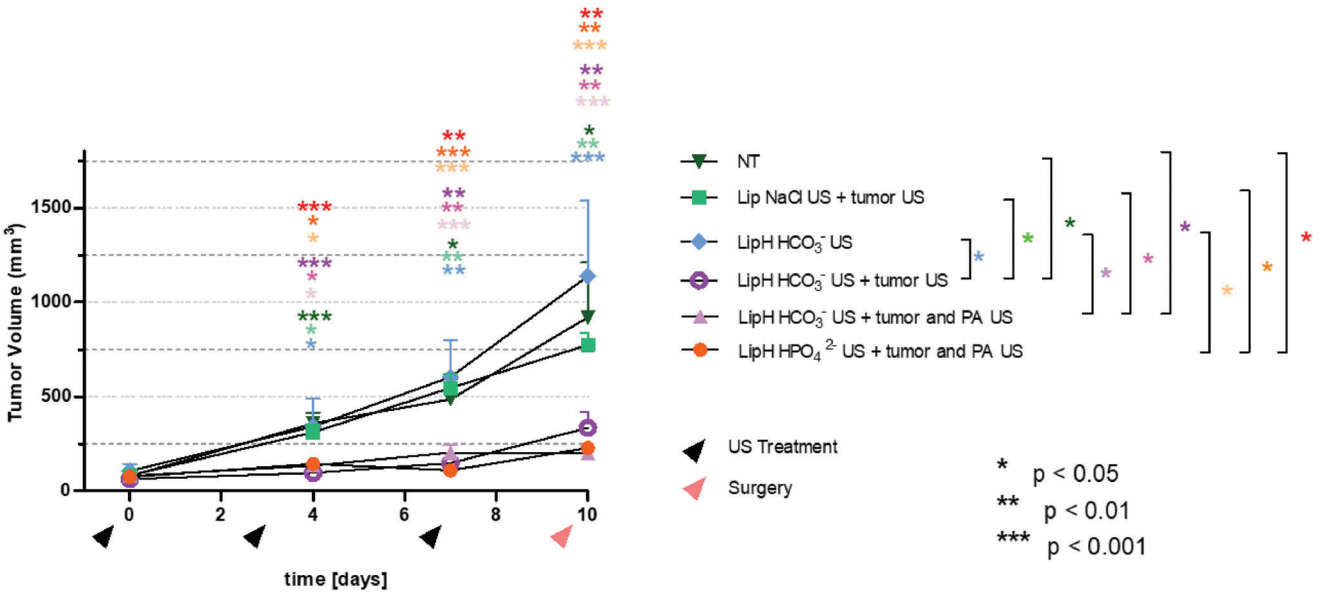

Figure 4. Tumor growth from day 0 to day 10. At day 0 the mass of the tumor is about 60 mm^3. i) COHORT 1(NT) mice not treated (NT, dark green triangle), ii) COHORT 2(LB) mice treated with lipHosomes loaded with bicarbonate without US-treatment (LipH HCO_3^- US, light green square), iii) COHORT 3(LNU) mice treated with empty LipHosomes and US treatment at the tumor (Lip NaCl US + tumor US, light blue rhombus); iv) COHORT 4(LBU) mice treated with sonosensitive lipHosomes loaded with bicarbonate with US treatment at the tumor (LipH HCO_3^- US + tumor US, violet circle), v) COHORT 5 (LBUA) mice treated with sonosentive lipHosomes loaded with bicarbonate with US treatment of the primary tumor and at the level of pulmonary artery (LipH HCO_3^- US + tumor and PA US, pink triangle), vi) COHORT 6(LPUA) mice treated with sonosensitive lipHosomes loaded with phosphate treated as in (v) (LipH HPO_4^{2-} US + tumor and PA US, orange full circle). Each experiment was repeated at least three times. The results were presented as mean ± standard deviation. Significant differences between two groups were assessed by unpaired Student's *t*-test. Statistical analyses of in vivo experiments were performed using GraphPad Prism software by two-tailed unpaired Student's *t*-test and one-way ANOVA with Newman–Keuls's test significance was settled at the 5% level. *p*-value < 0.05 was marked as *, *p*-value < 0.01 was marked as ** and *p*-value < 0.001 was marked as ***.

experiments that would allow the acquisition of the relevant information on the several involved effects. This task implied the set-up of six cohorts of animal models whose tumor growth was monitored over time during the application of the therapeutic protocol. The results are reported in **Figure 4**.

As shown in Figure 4, there was a significant difference in the tumor growth between controls and the properly treated cohorts, already four days after the beginning of the first treatment. Importantly, for the properly treated cohorts, the tumor masses did not show any significant growth over all the monitored time. It is also interesting to notice that among the properly treated cohorts there is no significant difference between lipHosomes containing bicarbonate and lipHosomes loaded with phosphate, thus supporting the view that the observed effect is due to the buffering capacity of the tumor microenvironment rather than to other effects of bicarbonate.

As a control of the successful release of bicarbonate by the lipHosomes following the application of the ultrasound pulse, both urine pH and extracellular tumor pH were measured. The urine was collected and the pH measurements were acquired ex vivo with a standard pH-meter. The pH of urine samples from treated mice showed an increase in respect to the values of the not treated ones, from 5.5 to 6.6 (Figure S4, Supporting Information). Anyhow it is worth noting that the observed increase still maintained the urine pH in its physiological range.

By using Iopamidol as pH MRI reporter, in vivo extracellular tumor pH was mapped pre- and post- US-treatment following the injection of sonosensitive lipHosomes loaded with bicarbonate (**Figure 5**).

The average extracellular tumor pH of triple negative 4T1 tumors before treatment was 6.86 ± 0.05. After the administration of LipHUS and the application of the ultrasound stimuli, a marked and statistically significant increase of tumor pHe values to 6.97 ± 0.10 was observed ($p < 0.05$, Figure 5B). Thus MRI CEST maps fully supports the view that extracellular tumor pH underwent a marked alkalinization upon the applied treatment (Figure 5A). By careful inspection on the frequency distribution of the tumor pHe values one clearly draw the conclusion that there is a net reduction of the number of pixels with acidic values and the corresponding increase of tumor pixels with less acidic (or more neutral) pH values after the treatment (Figure 5C).

2.4. Effect of the LipH/HCO_3^-/US Treatment on Tumor Recurrence after Surgery

On day 10, the primary tumor was surgery excised. On day 14 mice underwent to a new, combined LipH /HCO_3^-/US treatment with insonation applied in the area where the tumors were surgically resected in order to evaluate the efficacy of the treatment on tumor relapse. The same scheme of liposomes administration and insonation used for the primary tumor treatment was adopted. Again six mice cohorts were investigated. Just a minor change has been introduced as cohort COHORT

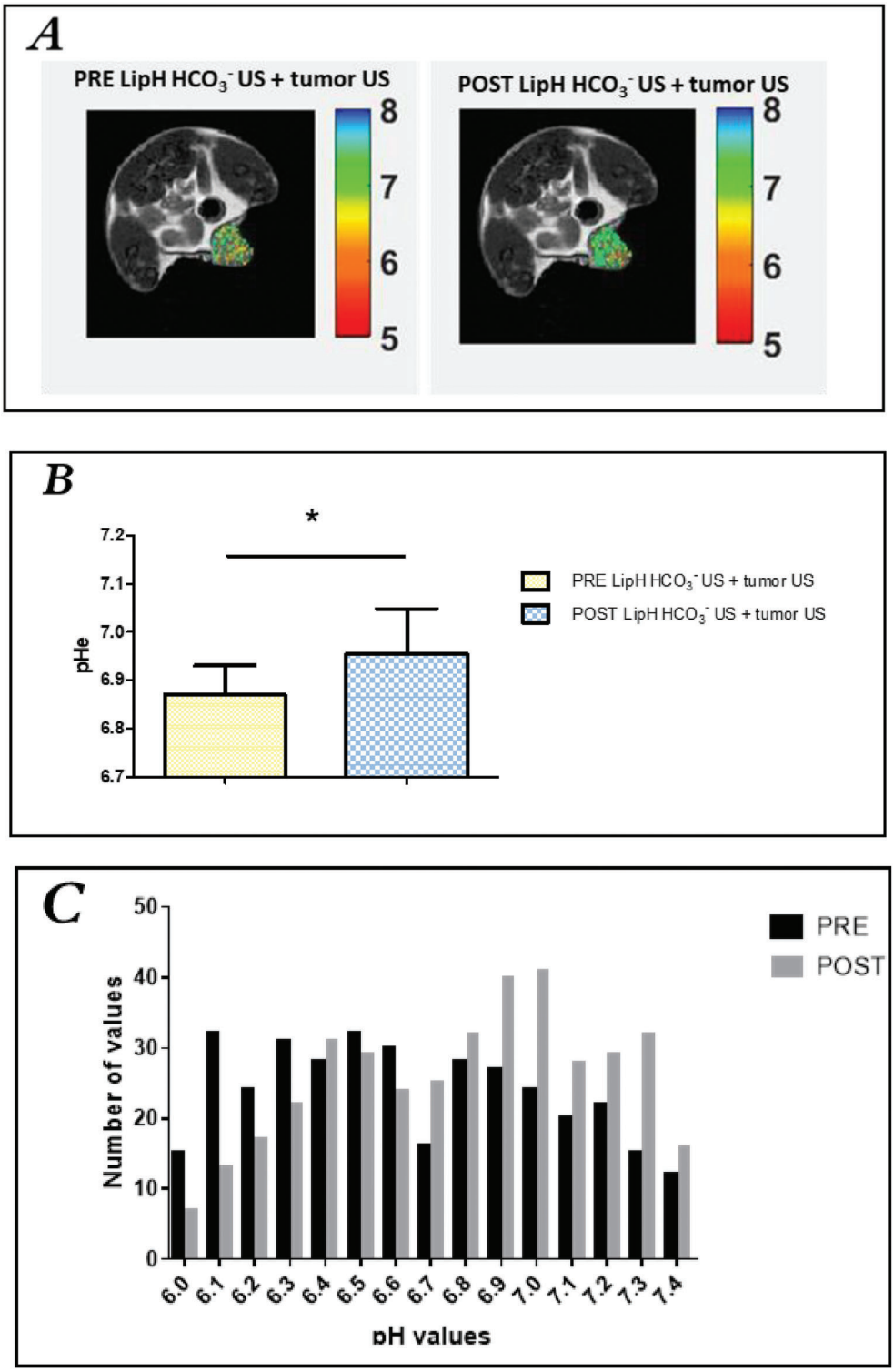

Figure 5. Assessment of tumor pHe changes by MRI-CEST imaging. A) Representative MRI-Iopamidol-CEST maps of extracellular tumor pH of 4T1 murine model before (left) and after (right) the treatment with sonosensitive lipHosomes loaded with bicarbonate (LipH HCO_3^-)) injected at the dose of 0.17 mmol kg^{-1} and ultrasound application at the tumor site. B) Quantification of averaged tumor pHe values (three mice) before and after US treatment with sonosensitive lipHosomes loaded with bicarbonate (LipH HCO_3^-). C) Histograms of voxel by voxel tumor pH values for a representative tumor (the one showed in panel B) before (PRE, black) and after (POST, gray) the treatment with sonosensitive lipHosomes loaded with bicarbonate (LipH HCO_3^-) and ultrasound application at the tumor site.

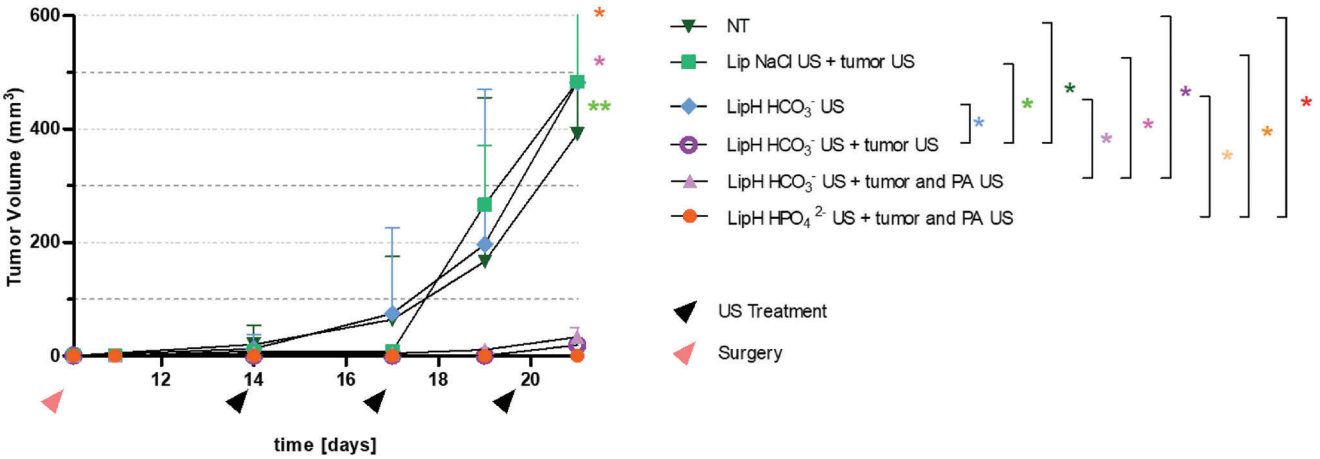

Figure 6. Tumor growth of 4T1 murine model after the surgical removal of the primary lesion; day 10 is the day of the surgery. i) COHORT 1(NT) mice not treated (NT, dark green triangle), ii) COHORT 2(LB) mice treated with sonosensitive lipHosomes loaded with bicarbonate without US-treatment (LipH HCO_3^- US, light green square), iii) COHORT 3(LNU) mice treated with empty liposomes and US applied at the tumor cavity(Lip NaCl US + tumor US, light blue rhombus); iv) COHORT 4(LBU) mice treated with sonosensitive lipHosomes loaded with bicarbonate with US treatment applied at the tumor cavity (LipH HCO_3^- US + tumor US, violet circle), v) COHORT 5 (LBUA) mice treated with sonosentive lipHosomes loaded with bicarbonate with US treatment applied at the tumor cavity and at the level of pulmonary artery (LipH HCO_3^- US + tumor and PA US, pink triangle), vi) COHORT 6(LPUA) mice treated with sonosensitive lipHosomes loaded with phosphate with US treatment applied at the tumor cavity and at the level of the pulmonary artery (LipH HPO_4^{2-} US + tumor and PA US, orange full circle). Each experiment was repeated at least three times ($n = 3$). The results were presented as mean ± standard deviation. Statistical analyses of in vivo experiments were performed using GraphPad Prism software by two-tailed unpaired Student's *t*-test and one-way ANOVA with Newman–Keuls's test. Significant differences between two groups were assessed by unpaired Student's *t*-test. Significance was settled at the 5% level. *p*-value < 0.05 was marked as *, *p*-value < 0.01 was marked as **, and *p*-value < 0.001 was marked as ***.

5 (LBUA) received US irradiation also at the level of pulmonary artery in addition to the tumor cavity The control cohorts (cohort 1(NT),2(LB),3(LNU)) showed that the recurrence of the tumor lesion was already detectable at day 17 followed by an exponential growth. In contrast, all the treated cohorts showed a very limited recurrence at the resected primary tumor site (**Figure 6**).

2.5. Effect of the Liposomes Loaded with HCO_3^- and US Treatment on Metastases Formation

There is ample evidence that the metastatic process is favored by the acidic pH at the extracellular tumor region.[19] Therefore, it is expected that the applied alkalinizing protocols might be effective also on preventing the metastatic process. As shown above, the increase of pH was pursued through an i.v. injection of liposomes containing a buffer solution at pH 10 and by applying an external ultrasound stimulus at the tumor region (cohort 4(LBU)) or by applying a double insonation both at the primary tumor lesion and at the level of the pulmonary artery (cohort 5(LBUA) and 6(LPUA)). The latter ultrasound stimulus was applied to assess whether the treatment was able to prevent the engraftment of circulating tumor cells at niches eventually characterized by an acidic pH. The metastases were visualized in vivo by anatomical T_{2w} MR image acquisition before the mice were sacrificed. As shown in **Figure 7**, healthy lungs filled with air showed no signal and appeared black in the MR image. On the contrary, the metastatic tissue resulted in high intensity globular signal scattered in the chest (Figure 7B,F). After the sacrifice, the lungs were stained by intra-tracheal injection of India ink. The strong negative charge on the tumor cell surface prevented ink from entering in the metastases and allowed the identification of the secondary tumor lesions (in white whereas the healthy pulmonary tissue was black) (Figure 7D,H). In order to enumerate macroscopic metastasis by ImageJ, the lungs of all mice cohorts were stained to be Imaged by MR T_{2w} images with slice thickness of 0.5 mm. The MR images acquired ex vivo on healthy lung tissue showed a higher signal intensity in respect to the signal arising from the underperfused metastatic tissue (Figure 7C,G). Finally the assessments of metastatic tissue were performed by histological analysis. (Figure 7E,I; Figure S3, Supporting Information). The US stimulus was not applied directly in the lungs because of the air, but in the blood stream at the pulmonary artery level. Histology acquired on mice at the end of the US treatment clearly showed that there are not alteration of the acinar lung architecture, as is shown in the microscopic images (Figure S6, Supporting Information).

As shown in the case of the cohort 4(LBU)), the treatment with LipHUS and ultrasound applied at the primary tumor site was, per se, able to significantly reduce the number of metastases compared to not treated mice (*p*-value < 0.05). However the additional insonation performed at the level of the pulmonary artery (treatment of cohorts 5(LBUA) and 6(LPUA)) had a further strengthening of this effect, that resulted particularly evident in the case of cohort 5(LBUA). The India Ink staining (Figure 7D,H) confirmed the different number of metastases as the histological staining (Figure 7E,I). An unexpected very high number of metastases were found for control mice of cohort 3(LNU) with respect to the not treated ones. This feature is worth being deepened but it is beyond the scope of this work and will be the subject of a new study.

The weight of all the mice involved in the study was measured each day over the three weeks of the study. No relevant weight loss

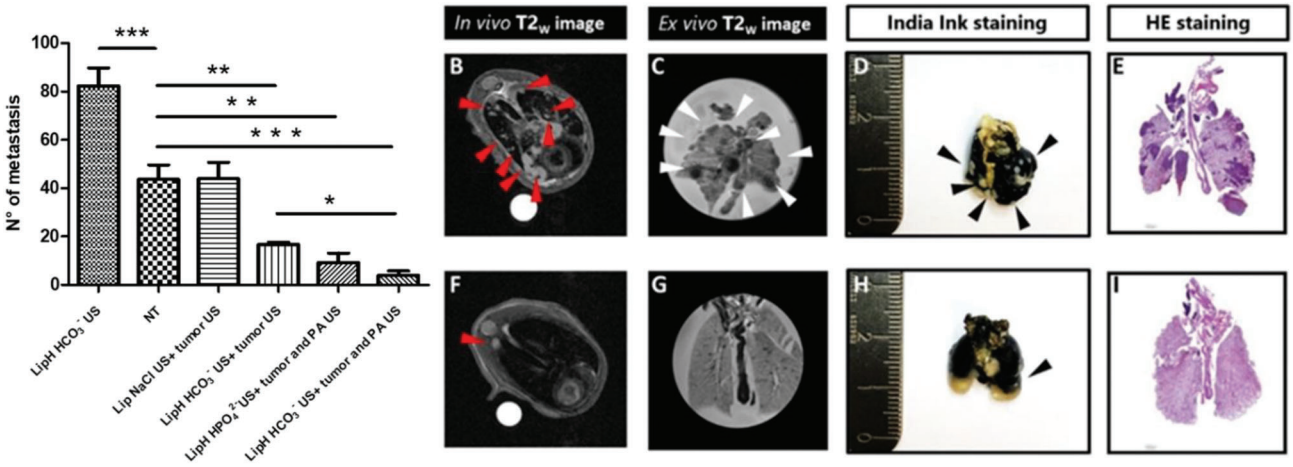

Figure 7. Effect of treatment on the metastases' formation process. A) The histograms report on the number of metastases detected at day 21 for each cohort. B) In vivo MRI T2w image of NT mice lungs (metastases indicated by red arrows). C) Ex vivo MRI-T2w of NT mice lungs (metastases indicated by white arrows). D) India Ink stained NT mice lung ex vivo (metastases indicated by black arrows). E) H&E stained NT mice lungs (metastases in dark violet). F) In vivo MRI-T_{2w} Image of mice lungs after treatment with LipHosome loaded with HCO_3^- and insonated at the tumor site and at the level of pulmonary artery (metastases indicated by red arrows). G) Ex vivo MRI-T2w image of mice lungs treated as in (F) (metastases indicated by white arrows). H) India Ink stained mice lungs ex vivo treated as in (F) (metastases indicated by black arrows). I) H&E stained mice lungs treated as in (F) (metastases in dark violet). Each experiment was repeated independently at least three times. The results were presented as mean ± standard deviation. Significant differences between two groups were assessed by unpaired Student's *t*-test. One-way ANOVA with Dunnett's post-hoc was performed to compare the metastases number of treated to the untreated group of and to compare the therapeutic effect of single ultrasound treatments to the double ultrasound applications. Significance was settled at the 5% level. *p*-value < 0.05 was marked as *, *p*-value < 0.01 was marked as **, and *p*-value < 0.001 was marked as ***.

was recorded for any investigated cohort (see Figure S3, Supporting Information).

3. Discussion

In this study we explored the possible therapeutic effect of microenvironment pH regulation i) on the primary tumor growth, ii) on its relapse, and iii) on its metastatic potential, in a TNBC murine model. It is a well-accepted view that the decrease in extracellular pH leads to an enhanced aggressiveness of the primary tumor and several studies have suggested how the action of a buffer is able to slowdown or reduce the tumor growth.[19,29,21,22] In this study, we investigated how bicarbonate encapsulated in stealth sonosensitive liposomes released at the sites of interest in a controlled manner can affect the tumor progression. In the used liposomal formulation, the pH of the internal solution is highly alkaline (pH 10) and the pH gradient with the external compartment is kept until the action of the US stimulus causes the release of the liposome's payload. The application of US to sonoliposomes definitively improves the bioavailability of the alkaline buffer loaded into the nanoparticles either when trapped in the extracellular matrix or flowing through the tumor vasculature. We decided to apply the US irradiation at the tumor region immediately after the i.v. injection to maximize the attainable increase of the local pH. The release of the alkaline payload is then maximized at the irradiated regions whereas the LipHosomes circulating in other body districts are not affected. Actually they act as an internal pool to supply bicarbonate/phosphate when they enter the US irradiation areas, that is, at the tumor region and/or at the regions identified as likely sites for the metastases' formation.

The 4T1 TNBC model was chosen in virtue of its ability to be an aggressive tumor phenotype similar to human breast cancer disease.[23,30–36] Moreover, it is known that the disease progression in the used model results spontaneously in pulmonary metastatic lesions.[23,33] Localized and controlled drug release by means of low intensity US has found interesting applications in recent years.[16,17] The transient permeabilization of these nanocarriers depends on properties of the overall composition of their membrane.[37,24] The membrane composition used for this study (DPPC/DSPC/Chol/DSPE-PEG-2000 molar ratio 10:5:4:1) was already used to generate liposomes sensitive to low intensity pulsed ultrasound.[25] The liposomes used in this work are not only sonosensitive but are also able to maintain a pH gradient between intra and extra liposomal medium for a time well sufficient for the intended application. This type of liposomes has been already described for applications in in vitro ligand anti-ligand test where they have been named LipHosomes.[26] A good prediction of the in vivo stability of liposomes can be obtained by studying the in vitro behavior in serum at 37 °C. The aim was to check the stability of the pH gradient as the passage of H_3O^+ through the membrane could, in principle, be easier than other solutes. We have observed that a stability of the pH gradient in physiological condition is granted for the first 30 min followed by a slow increase (Figure 2). In the herein proposed therapeutic protocol, the objective is to maintain the pH gradient in vivo until liposomes are induced to release their payload upon the application of US stimuli in the region of interest. The US stimulus is therefore applied immediately after the i.v. injection of the liposomes in order to maximize the pH variation in the insonated area. In order to verify that the release has occurred, we performed in vivo pH measurement in the tumor area before and after the

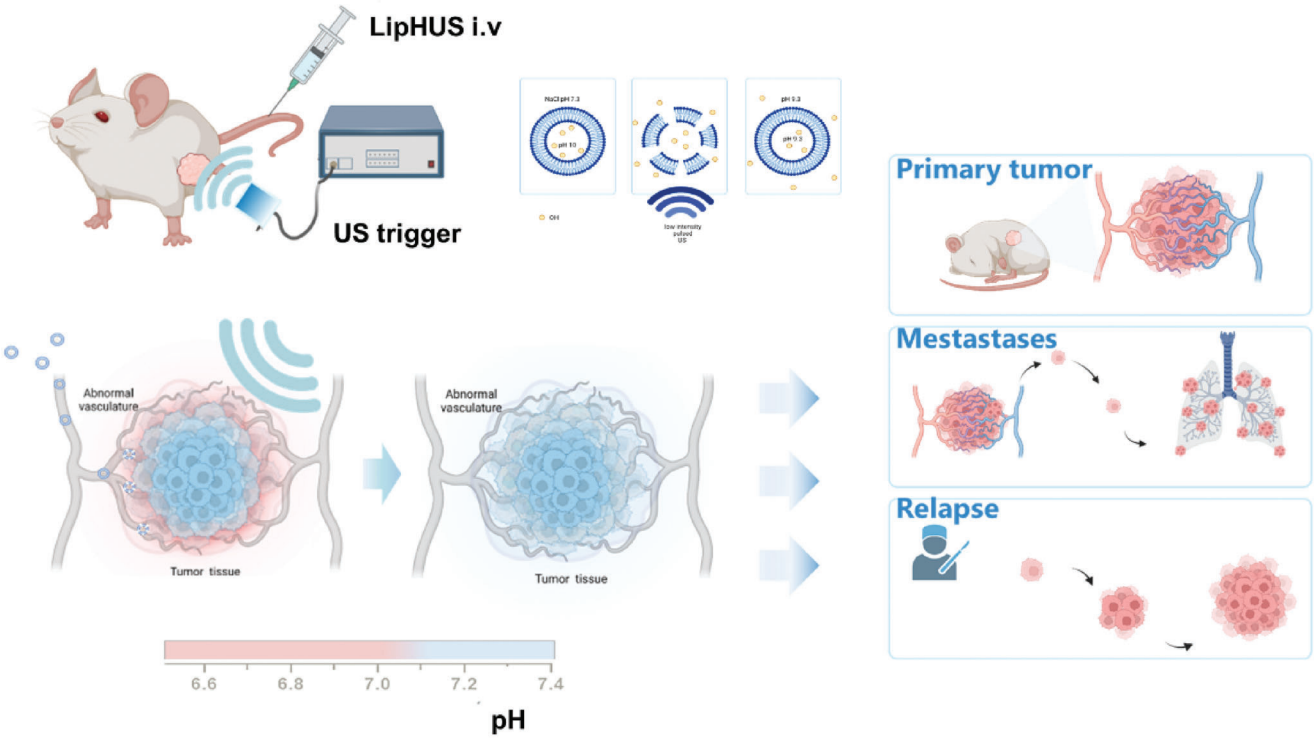

Figure 8. Scheme of the in vivo experiments. The aim of this study is the modification of pH in tumor extracellular microenvironment and the assessment of the effects on the growth of the primary tumor, on metastases formation and on the recurrence of lesions at the site of the primary tumor. Before applying the therapeutic protocol, we waited for the tumor volume to reach 60 mm^3. Local tumor insonation, performed immediately after liposome injection, was repeated three times every four days prior to surgical resection of the tumor, which occurred on the tenth day from the start of the therapeutic protocol. After the surgery, the treatment was repeated three times every four days, either in the operated area or in the pulmonary artery, in order to induce an increase in pH in the lungs as well.

administration of the LipH suspension and application of the US stimuli. Although a wide range of imaging techniques[27] are available for assessing tumor pH in vivo, MRI appears the most suitable one for the highest temporal and anatomical resolution. Among the MRI techniques, MRI-CEST tumor pH imaging with Iopamidol showed to be a useful tool to map tumor acidosis and pH modifications after therapeutic treatments. The method is endowed with high spatial resolution and allows to assess the heterogeneity of extracellular acidification.[18,28] In vivo experiments showed a marked and significant increase of the tumor pH before and after the treatment with LipH-US, with a clear shift from more acidic to less acidic tumor pH values inside the whole tumor region. Further evidence of the payload release from liposomes upon insonation is provided by the measurements of pH in the urine (Figure S4, Supporting Information). An increase in pH from 5.5 to 6.5 was observed within the first two hours after the insonation of liposomes.

The treatment, consisting of an i.v. injection of lipHosomes followed by the application of US for 90 s at the tumor region (**Figure 8**), started when the tumor volume reached 60 mm^3 and was repeated three times during the following ten days (**Scheme 1**). During this period the size of the tumor lesions was measured for all mice. For those cohorts that have received the alkalinizing protocols the primary tumor growth has been markedly slowed down, apparently some of them seemed to stop growing at all (Figure 4). This observation is in agreement with what reported by Abumanhal-Masarweh et al.[37] who reported that the combined treatment of triple-negative breast cancer cells (4T1) with doxorubicin and sodium-bicarbonate enhanced drug uptake and increased its anti-cancer activity. Doxorubicin as ionizable weak-base freely permeates membranes in its uncharged form. In acidic environments, weak bases become charged and their permeability through the phospholipidic bilayer is inhibited. The bicarbonate was brought to the tumor region by LipHosomes and showed to accumulate at the extracellular space due to the known EPR effect. In an in vitro experiment it was shown that the effect of free bicarbonate was greater than that observed for the entrapped bicarbonate thus suggesting that the bicarbonate action is effective when outside the cells. Moreover, upon carrying out US imaging, the authors surmised the formation of CO_2 from the liposomal bicarbonate as the increased contrast was assigned to the CO_2 gas detectable by ultrasonic imaging. Along this line of reasoning a liposome encapsulating NH_4HCO_3 solution was investigated as Photo Acoustic Imaging contrast agent whose enhanced response relies on the formation of CO_2 which swells under specific optical laser wavelengths.[39]

Another interesting approach to increase pH in the tumor ECM was made by administering vaterite $CaCO_3$ nanoparticles whose dissolution is determined by the $[H^+]$.[40] The lower pH of the ECM in the tumor region yields the formation of Ca^{2+} and CO_3^{2-} ions. The latter ones enter the equilibrium reaction with bicarbonate and, in turn, with H_2CO_3 that decomposes to

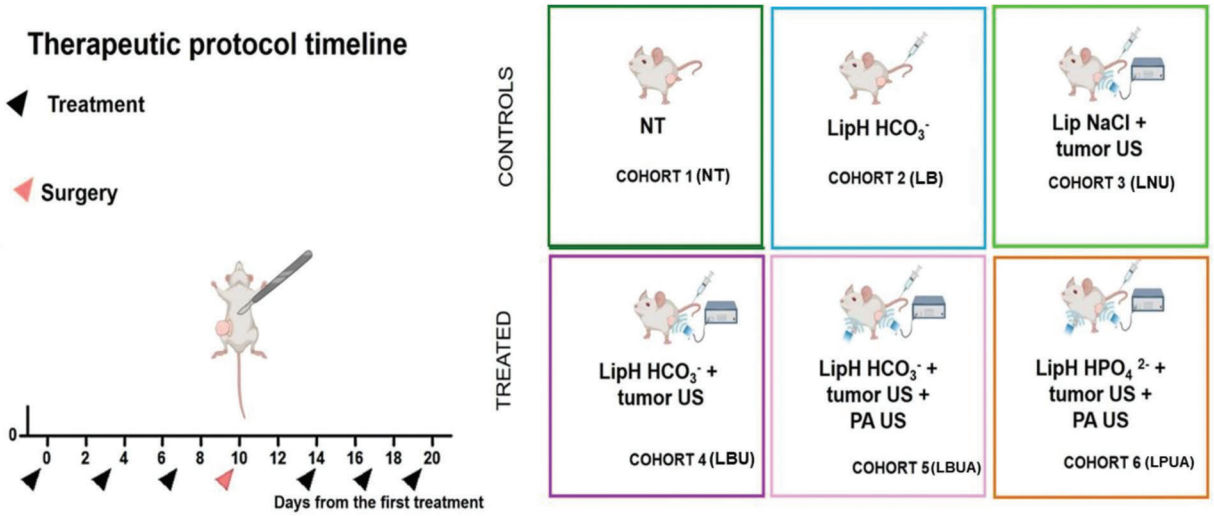

Scheme 1. Schematic description of the therapeutic protocol timeline and of the Mice cohorts. The control mice group was divided into three subgroups: i) untreated mice (NT), COHORT 1(NT), ii) mice treated with sonosensitive liposomes loaded with sodium bicarbonate (LipH HCO_3^-, indicated as LB in the identification name of the cohort), no insonation, COHORT 2(LB), iii) mice administered with sonosensitive liposomes loaded with NaCl (Lip-NaCl, indicated as LN in the identification name of the cohort) and treated with ultrasound (insonation in situ will be referred as U in the identification name of the cohort) COHORT 3 (LNU). In the second group, the tumor bearing mice were divided into three subgroups: i) mice injected with lipH HCO_3^- and insonated on the primary tumor mass, COHORT 4(LBU), ii) mice treated with LipH HCO_3^- and subjected to ultrasonic treatment on the tumor and on the pulmonary artery (insonation in the pulmonary artery will be referred as A in the identification name of the cohort), COHORT 5(LBUA), iii) mice treated with liposome incapsulating sodium phosphate at pH 10.0 instead of HCO_3^- (Lip HPO_4^{2-}, referred as LP in the identification name of the cohort) with a double insonation, first on the tumor and then on the pulmonary artery, COHORT 6(LPUA).

water and CO_2. The attained ΔpH value of 0.2 unit was measured with a 0.5 mm invasive in vivo pH electrode probe upon using nanoparticles of 100 nm diameter. The administration of $CaCO_3$ nanoparticles resulted in a significant inhibition of tumor growth. However, discontinuation of the nano-$CaCO_3$ treatment partially reversed this trend, resulting in the acceleration of the tumor growth rate. Clearly an improved control of the alkalinization procedure at the tumor region appears necessary but the obtained results further supports the view that the alkalinization approach is a valuable one. Furthermore a more accurate method to assess the extracellular pH is needed as the assumption that the observed pH value from the invasive electrode probe could be assigned to the pH of the extracellular space is largely tentative.

To evaluate whether the therapeutic effect on the tumor growth has to be associated to the pH rise and not on to an effect of the microbubbles of CO_2 that could form from bicarbonate release, we tested liposomes in which bicarbonate was replaced by phosphate buffer. The combination of LipHUS HPO_4^{2-} and low intensity pulsed ultrasound seems to be effective as the combination of LipHUS HCO_3^-, as shown with cohort 5(LBUA) and 6(LPUA). This finding clearly indicates that the pH buffering is the main cause for the observed effect on the growth of the primary tumor.

The main issue in translating the use of buffers into the clinic was related to the large dose to be administered. Our preclinical work shows that with the localized delivery it is possible to reduce by 300 times the dose and obtain very good therapeutic effects. It is straightforward to say that reducing the dose will reduce possible side effects and it may limit what several articles reported on the occurrence of systemic alkalosis following the oral buffer treatment. In some cases a pH of 9 was measured in the urine.[41,42] On the contrary, in our study the urine pH of treated mice was never higher than 6.5 until few hours after the treatment (Figure S4, Supporting Information).

The remarkable results obtained by applying this treatment on primary tumor, led us to test its efficacy on the recurrence and metastatic events, that are the leading causes of poor prognosis in triple negative breast cancer. The TNBC is characterized by having a 5-years overall survival rate that is significantly lower than the other subtypes of breast cancer, with an early peak of recurrence.[34,35] Thus, a localized treatment to avoid the recurrence of this type of tumor is most of need. Despite all the progress made in molecular characterization and classification of breast cancer into various subtypes, the heterogeneity in response to standard chemotherapy regimens makes it difficult to identify a signaling pathways or oncogenes target that can be used to escape the relapse.[36] Therefore, using pH as targeted therapy seems to be an approach able to act on different key functional nodes.[43] In this study, mice of cohort 4(LBU), 5(LBUA) and 6(LPUA), were continued to be treated even after surgery. Very delayed recurrence or no recurrence at all was observed during ten days after the surgery whereas control groups displayed an evident tumor recurrence already at the 7th day after surgery and at day 10th after surgery the tumor masses have already reached a volume of 500 mm^3 (Figure 6). These results prove that controlled release of buffer in the tumor might be a non-invasive, reliable method to fight the recurrence. There are several mechanisms that can contributes to the success of therapy, indeed, the bicarbonate therapy was associated with increased T-cell infiltration, that is correlated with good prognosis in different solid cancers.[40,44] Another mechanism that seems to be pivotal in carcinogenesis progression is the autophagy, regulating the maintenance of cancer stemness and inducing the tumor recurrence.[45–47] Recently, the increase of pH has been related

also with alterations in the cells autophagy.[48] Finally the third level we wanted to test the efficacy of the herein proposed therapeutic protocol is on the possibility of controlling the metastases spread out.

It has been reported that increasing the primary tumor pH is expected to decrease the tumor metastatization activity. Several reports demonstrated that tumor acidic pH contribute to provide a hostile environment in the peritumoral healthy tissues, resulting in extracellular matrix degradation, altered angiogenesis, and immune response suppression.[49–54] Therefore, the use of a method to buffer the acidic pH through the systemic administration of buffers was used to reduce lung metastasis with a positive outcome.[10,55,56] However, mixed results were obtained with this approach in different tumor murine models.[57] A recent study, on the same murine tumor model used in this work, reported that the treatment ad libitum with 200 mM of bicarbonate buffer did not provide any effect in the number of lung metastasis.[58] The herein proposed protocol, where two insonations are conceived to trigger a local bicarbonate release in the tumor region and at the level of pulmonary artery, appears to represent a possible improvement with respect to the previous buffer administration protocols. The insonation of the pulmonary artery region had the scope to alter the pH in the lungs, that is the organ most involved in 4T1 tumor metastasis, thus preventing the engraftment of blood circulating tumor cells. It is worth noting that the number of lung metastases is significantly reduced even for mice belonging to the cohort 4(LBU) that received a single insonation on the primary tumor compared to not treated mice. Cohort 5(LBUA) and 6(LPUA), that have received the second insonation, displayed a reduction in lung metastasis formation even more significant and some mice of this groups have not developed any metastasis at all. Finally it was found that no difference in the therapeutic outcome was observed for 5(LBUA) and 6(LPUA) protocols, thus indicating that PBS buffer or bicarbonate buffer could be indifferently used for the herein proposed method (Figure 7).

4. Conclusions

In this study we have presented promising results showing a nearly complete tumor healing for a TNBC murine model upon treatment with localized alkalinizing therapy. The therapeutic protocol consists in the administration of buffer at high pH, encapsulated into sonosensitive liposomes, followed by the application of low frequency ultrasound in the tumor region and at the pulmonary artery. The liposomes administration was performed three times during the primary tumor growth and two times after tumor surgery. Mice under treatment showed a remarkable effect on the growth of the primary tumor lesion. In several cases it was found that the treatment led to a full stop in the tumor growth. After the surgery, treated mice displayed no recurrence and the number of metastasis was very low with respect to the control groups. Even though similar results were already anticipated for alkalinizing therapy, this protocol requires a dose 300 times lower with respect to therapy performed by oral or intravenous buffer administration. Moreover, no systemic alkalinization occurs. The low dose of buffer required for this treatment seems to be an excellent starting point for translating this therapy into the clinic. From these preclinical observations it is not possible to state whether the therapeutic protocol could be fully efficient on its own or will be useful only as support to conventional therapy. Clinical trials were recently carried out based on the transarterial chemoembolization (TACE) to deliver doxorubicin-lipiodol emulsion and oxaliplatin/homocamptothecin and at the same time embolize the tumor feeding arteries, in combination or not with bicarbonate within the tumor.[59] This clinical trial showed that the presence of the buffering treatment brought an improved anticancer activity of TACE. This strategy might be further implemented by the use of herein described LipHUS. Finally we think that an important achievement of this work consists in the identification of a novel approach to avoid the recurrence of triple negative breast cancer after surgical removal. Being the small buffering doses involved and the noninvasive characteristics of the treatment, the herein reported procedure may be considered for clinical translations by breast tumor surgeons.

5. Experimental Section

Liposomes Preparation: The ultrasound-sensible phospholipidic film was prepared as described by Rizzitelli et al.[25] Briefly, all the phospholipids used were purchased from Avanti Polar Lipid Inc. (Alabaster, AL, USA), whereas all other chemicals were from Sigma-Aldrich (Milano, Italy). DSPE-PEG-2000- methoxy, DPPC, DSPC, and Cholesterol (molar ratio DPPC/DSPC/Chol/DSPE-PEG-2000-methoxy 10:5:4:1, 40 mg mL^{-1}) were dissolved in chloroform and then dried under rotation in a rotavapor system for 2 h. The film formed on the balloon wall was further dried under vacuum for 4 h. In this study the thin phospholipidic film was hydrated at 55 °C with:

i. sodium bicarbonate 150 mM (basified with NaOH to pH 10.0) (LipH HCO_3^-) or with
ii. sodium phosphate 100 mM (basified with NaOH to pH 10.0) (LipH HPO_4^{2-}) using the method reported by Tripepi et al.[26] or with
iii. NaCl 0.15 M (Lip NaCl).

The former two liposomes contained buffers at high concentration and could maintain a pH gradient between intra and extra liposomal medium whereas the third had no pH gradient between intra and extraliposomal space, as observed by Tripepi et al.[26]

To generate nanocarriers of defined and uniform size, they were extruded by passing the liposome suspension through a polycarbonate membrane filter with pores of decreasing size (800 nm, 400 nm, 200 nm, 100 nm). The final suspension of vesicles was purified by exhaustive dialysis carried out at 4 °C against 0.15 M NaCl aqueous solution at pH 7. The vesicles were characterized by using DLS (Zetasizer NanoZS, Malvern, UK) to define the mean hydrodynamic diameter and the polydispersity of the system.

In Vitro Release Experiments: In order to assess the payload release potential, the liposomes' suspensions were either heated or treated with US and the results were compared. To assess the thermal activation of the content release, the nanovesicles suspension, diluted 1:10 in NaCl 0.15 M in phosphate buffer saline (PBS) or in human serum (HS), were heated at 55 °C for 15 min. To follow the release induced by ultrasound, the liposomes' suspension was diluted in the various buffers and insonated for 1.5 min at different acoustic pressure. Low intensity pulsed ultrasound was generated using 1 MHz transducer (Precision Acoustics, UK). The pulsed mode was managed by wave generator set on burst mode (duty cycle (DC) 50%, pulse repetition frequency (PRF 4 Hz)), connected to a power amplifier 50 dB.

Mouse Model: For in vivo experiment BALB/C 7 week-old female were purchased from Charles River Laboratory (USA) and maintained in standard condition according to the European directive 2010/63 on the protection of animals used for scientific purposes and transposed on Legislative Decree 26/2014. All in vivo experiments were accomplished with the prior approval of Italian Ministry of Health (Experimental

protocol authorization n. 63/2016-PR, released on 03/03/2017 for protocol n. 21658.EXT.4).

To obtain breast mouse model, mice were injected subcutaneously with 1×10^4 4T1 cells.

The 4T1 breast cancer cell line metastatic processes followed the onset of the primary tumor lesion. The metastases occurred via a hematogenous route to liver, lungs, bone, and brain. The 4T1 cells grew aggressively and caused a uniformly lethal disease even after excision of the primary tumor. The application of the therapeutic protocol started when the tumor reached the volume of about 60 mm^3. Local tumor insonation, performed immediately after liposome injection, was repeated three times every four days prior to surgical resection of the tumor, which occurred on the tenth day from the start of the therapeutic protocol. After the surgery, the treatment was repeated three times every four days, either in the surgical cavity or at the level of the pulmonary artery. The aim was to induce an increase in pH in the lungs being this organ a well-established target for metastases in this type of breast cancer model.

In Vivo Experiments—Cohorts Description: After ten days, mice with a tumor volume of 60 mm^3 ($\pm$10) were recruited and divided in 6 cohorts. In particular, mice were divided into 2 groups (control and properly treated ones) and each group was further divided into 3 subgroups for a total of 6 mice for each cohort (Scheme 1) The 3 control subgroups were as follows: i) untreated mice (NT), COHORT 1(NT), ii) mice treated with sonosensitive lipHosomes loaded with sodium bicarbonate (LipH HCO_3^-, indicated as LB cohort), no insonation, COHORT 2(LB), iii) mice administered with sonosensitive lipHosomes loaded with NaCl (Lip-NaCl, indicated as LN in the identification name of the cohort) and treated with ultrasound (insonation in situ will be referred as U in the identification name of the cohort) COHORT 3 (LNU).

In the second group, the tumor bearing mice were divided into 3 subgroups: i) mice injected with lipH HCO_3^- and insonated on the primary tumor lesion, COHORT 4(LBU), ii) mice treated with LipH HCO_3^- and subjected to ultrasonic treatment on the tumor and on the pulmonary artery (insonation in the pulmonary artery will be referred as A in the identification name of the cohort), COHORT 5(LBUA), iii) mice treated with lipHosome encapsulating sodium phosphate at pH 10.0 instead of HCO_3^- (Lip HPO_4^{2-}, referred as LP in the identification name of the cohort) with a double insonation, first on the tumor and then on the pulmonary artery, COHORT 6(LPUA).

The involvement of the last group was deemed useful in order to assess that the observed effect was associated to the buffering capacity induced by the release of the basic payload from the insonated liposomes rather than other unknown mechanism (Scheme 1).

Treatments were performed every four days for 10 days and the tumor growth was measured by caliper ($D \times d^2/2$; D = longer diameter, d = shorter diameter).

In Vivo Experiments—Protocol for In Vivo Local Insonation: In order to perform in vivo release of LipHosomes, the skin of the used BALB/C mice was shaved in the local areas one day before the treatment. The piezoelectric transducer was placed on the skin at the tumor region or at the level of the pulmonary artery and ultrasound gel was used as ultrasonic waves transmission medium. The low intensity pulsed ultrasound was applied for 90 seconds at the intensity of 2 W cm^{-2} and the acoustic pressure of 0.25 MPa immediately after the injection of 0.17 mmol kg^{-1} sodium bicarbonate loaded in liposomes. The area involved in the treatment did not show ultrasound-induced damage, according to mechanical index that was estimated at 0.25. The therapeutic protocol was designed as follows: mice with 60 mm^3 mass volume were enrolled in the experiment, the treatment was performed on days 0, 3, and 7 and the effect of the treatment on the primary tumor growth was evaluated by caliper measurements. The treatment consisted of the i.v. administration of lipHosomes at the dose of 0.17 mmol kg^{-1} $NaHCO_3$ (corresponding to 0.3 mmol kg^{-1} of phospholipids) followed by the application of low frequency US directly on the tumor mass and at the pulmonary artery to induce a pH increase in the lungs, where this type of tumor is known to metastatize, thus creating an unfavorable engrafting environment (Figure 8). This treatment was repeated three times during ten days. On tenth day the tumor was surgically explanted. Four days after the surgery, the mice were again treated with lipHUS and insonated in the surgical area on day 14, day 17, and day 19. The purpose of the applied treatment was to prevent the tumor recurrence after surgery. On day 21 the mice were sacrificed. The effect of the treatment on metastases formation was evaluated 21 days after the first liposomal administration (day 0).

In Vivo Experiments—In Vivo MRI pH Mapping of the Tumor Microenvironment: MRI-CEST images were acquired on a Bruker Advance Neo (Bruker BioSpin, Ettlingen, Germany) 7T MRI scanner equipped with a quadrature 1H coil. As reported by Longo et al.,[60] Z-spectra were acquired using a multi-slice single-shot RARE sequence with centric encoding (typical setting TR/TE/NEX = 11 000 ms/4.1 ms/1) preceded by a 3 μT cw block presaturation pulse for 5 s and by a fat-suppression module. A series of 47 frequencies were saturated to acquire a CEST spectrum in the frequency offset range $\pm$10 ppm. Eight slices were acquired with a slice thickness = 1.5 mm and an acquisition matrix of 96×96 reconstructed to 128×128 with a field of view of 30×30 mm^2 (in-plane spatial resolution = 234 μm).

MR-CEST images were repeated two times, before and after Iopamidol intravenous injection (dose = 4 g Iodine/(kg body weight)) before the US treatment and then repeated again right after the US treatment with a second dose of Iopamidol (dose = 0.8 g Iodine/(kg body weight)).

All CEST images were analyzed using in-house scripts implemented in MATLAB (The Mathworks, Inc., Natick, MA, USA).[60] Briefly, the Z-spectra were interpolated, on a voxel-by-voxel basis, by smoothing splines, B0-shift corrected and saturation transfer efficiency (ST%) was measured by punctual analysis. Difference contrast maps (ΔST%) were calculated by subtracting the CEST contrast after iopamidol injection from the CEST contrast before the injection on a per voxel basis to reduce the confounding effect of the endogenous contributions. Extracellular tumor pH (pHe) values were calculated in vivo by applying the ratiometric procedure and the calculated tumor pHe maps were superimposed onto the anatomical reference image.

Statistical Analysis: Each experiment was repeated independently three times. The results were presented as mean $\pm$ standard deviation. Statistical analyses of in vivo experiments were performed using GraphPad Prism software by two-tailed unpaired Student's *t*-test and one-way ANOVA with Newman–Keuls's test. One-way ANOVA with Dunnett's post-hoc was performed to compare the metastases number of treated to the untreated group of and to compare the therapeutic effect of single ultrasound treatments to the double ultrasound applications.

Significant differences between two groups were assessed by unpaired Student's *t*-test. Significance was settled at the 5% level. p-value < 0.05 was marked as *, p-value < 0.01 was marked as **, and p-value < 0.001 was marked as ***.

Supporting Information

Supporting Information is available from the Wiley Online Library or from the author.

Acknowledgements

S.A. and L.C. kindly acknowledge the support from National Key Research & Development Project, the Ministry of Science and Technology of China (No. 2018YFE0118800), National Natural Science Foundation of China (82025019, 82227806).

Conflict of Interest

The authors declare no conflict of interest.

Data Availability Statement

The authors will provide data when requested.

Keywords

bicarbonate, breast cancer, liposomes, microenvironment pH, recurrence treatment, ultrasound

Received: June 14, 2023
Revised: September 12, 2023
Published online:

[1] S. Łukasiewicz, M. Czeczelewski, A. Forma, J. Baj, R. Sitarz, A. Stanisławek, *Cancers* **2021**, *13*, 4827.
[2] N. Radosevic-Robin, P. Selenica, Y. Zhu, H. H. Won, M. F. Berger, L. Ferrando, E. Cocco, M. Privat, F. Ponelle-Chachuat, C. Abrial, J.-M. Nabholtz, F. Penault-Llorca, J. S. Reis-Filho, M. Scaltriti, *npj Breast Cancer* **2021**, *7*, 124.
[3] R. Dent, M. Trudeau, K. I. Pritchard, W. M. Hanna, H. K. Kahn, C. A. Sawka, L. A. Lickley, E. Rawlinson, P. Sun, S. A. Narod, *Clin. Cancer Res.* **2007**, *13*, 4429.
[4] N. M. Almansour, *Front. Mol. Biosci.* **2022**, *9*, 2296.
[5] P. H. Maxwell, G. U. Dachs, J. M. Gleadle, L. G. Nicholls, A. L. Harris, I. J. Stratford, O. Hankinson, C. W. Pugh, P. J. Ratcliffe, *Proc. Natl. Acad. Sci. U. S. A.* **1997**, *94*, 8104.
[6] E. Persi, M. Duran-Frigola, M. Damaghi, W. R. Roush, P. Aloy, J. L. Cleveland, R. J. Gillies, E. Ruppin, *Nat. Commun.* **2018**, *91*, 2997.
[7] N. J. Toft, T. V. Axelsen, H. L. Pedersen, M. Mele, M. Burton, E. Balling, T. Johansen, M. Thomassen, P. M. Christiansen, E. Boedtkjer, *eLife* **2021**, *10*, 68447.
[8] B. A. Webb, M. Chimenti, M. P. Jacobson, D. L. Barber, *Nat. Rev. Cancer* **2011**, *11*, 671.
[9] R. A. Gatenby, R. J. Gillies, *Nat. Rev. Cancer* **2008**, *8*, 56.
[10] I. F. Robey, B. K. Baggett, N. D. Kirkpatrick, D. J. Roe, J. Dosescu, B. F. Sloane, A. I. Hashim, D. L. Morse, N. Raghunand, R. A. Gatenby, R. J. Gillies, *Cancer Res.* **2009**, *69*, 2260.
[11] R. A. Gatenby, R. J. Gillies, *Nat. Rev. Cancer* **2004**, *411*, 891.
[12] M. Damaghi, R. Gillies, *Cell Cycle* **2017**, *16*, 1739.
[13] E. V. Zagaynova, I. N. Druzhkova, N. M. Mishina, N. I. Ignatova, V. V. Dudenkova, M. V. Shirmanova, *Adv. Exp. Med. Biol.* **2017**, *1035*, 105.
[14] S. Fais, G. Venturi, B. Gatenby, *Cancer Metastasis Rev.* **2014**, *33*, 1095.
[15] F. E. Díaz, E. Dantas, J. Geffner, *Mediators Inflammation* **2018**, *2018*, 1218297.
[16] A. Y. Rwei, J. L. Paris, B. Wang, W. Wang, C. D. Axon, M. Vallet-Regí, R. Langer, D. S. Kohane, *Nat. Biomed. Eng.* **2017**, *18*, 644.
[17] M. Amrahli, M. Centelles, P. Cressey, M. Prusevicius, W. Gedroyc, X. Y. Xu, P.-W. So, M. Wright, M. Thanou, *Nanotheranostics* **2021**, *5*, 125.
[18] C. Ward, J. Meehan, M. E. Gray, A. F. Murray, G. J. Argyle, I. H. Kunkler, et al., Explor Target Antitumor Ther **2020**, *1*, 71.
[19] S. R. Pillai, M. Damaghi, Y. Marunaka, E. P. Spugnini, S. Fais, R. J. Gillies, *Cancer Metastasis Rev.* **2019**, *38*, 205.
[20] V. Estrella, T. Chen, M. Lloyd, J. Wojtkowiak, H. H. Cornnell, A. Ibrahim-Hashim, K. Bailey, Y. Balagurunathan, J. M. Rothberg, B. F. Sloane, J. Johnson, R. A. Gatenby, R. J. Gillies, *Cancer Res.* **2013**, *73*, 1524.
[21] A. Ibrahim-Hashim, V. Estrella, *Cancer Metastasis Rev.* **2019**, *38*, 149.
[22] S. Harguindey, K. Alfarouk, J. P. Orozco, S. Fais, J. Devesa, *Int. J. Mol. Sci.* **2020**, *21*, 7475.
[23] B. A. Pulaski, S. Ostrand-Rosenberg, *Curr. Protoc. Immunol.* **2000**, *39*, 2021.
[24] D. Patrucco, E. Terreno, *Front. Phys.* **2020**, *8*, 325.
[25] S. Rizzitelli, P. Giustetto, J. C. Cutrin, D. Delli Castelli, C. Boffa, M. Ruzza, V. Menchise, F. Molinari, S. Aime, E. Terreno, *J. Controlled Release* **2015**, *202*, 21.
[26] M. Tripepi, P. O. Bennardi, G. Ferrauto, S. Aime, D. D. Castelli, *Anal. Sens.* **2021**, *1*, 48.
[27] L. Q. Chen, M. D. Pagel, *Adv. Radiol.* **2015**, *2015*, 206405.
[28] A. Anemone, L. Consolino, F. Arena, M. Capozza, D. L. Longo, *Cancer Metastasis Rev.* **2019**, *38*, 25.
[29] L. Yang, L. Yong, X. Zhu, Y. Feng, Y. Fu, D. Kong, W. Lu, T.-Y. Zhou, *J. Pharmacokinet. Pharmacodyn.* **2020**, *47*, 105.
[30] P. Kau, G. M. Nagaraja, H. Zheng, D. Gizachew, M. Galukande, S. Krishnan, A. Asea, *BMC Cancer* **2012**, *12*, 115.
[31] K. Tao, M. Fang, J. Alroy, G. G. Sahagian, *BMC Cancer* **2008**, *8*, 228.
[32] S. Yang, J. J. Zhang, X. Y. Huang, *Methods Mol. Biol.* **2012**, *928*, 221.
[33] F. C. Geyer, F. Pareja, B. Weigelt, E. Rakha, I. O. Ellis, S. J. Schnitt, J. S. Reis-Filho, *Am. J. Pathol.* **2017**, *187*, 2139.
[34] H. Kennecke, R. Yerushalmi, R. Woods, M. C. U. Cheang, D. Voduc, C. H. Speers, T. O. Nielsen, K. Gelmon, *J. Clin. Oncol.* **2010**, *28*, 3271.
[35] Q. Wu, S. Siddharth, D. Sharma, *Cancers* **2021**, *13*, 3697.
[36] R. C. Warren, *Physics and the Architecture of Cell Membranes*, CRC Press, Boca Raton, FL **1987**.
[37] H. Abumanhal-Masarweh, L. Koren, A. Zinger, Z. Yaari, N. Krinsky, G. Kaneti, N. Dahan, Y. Lupu-Haber, E. Suss-Toby, E. Weiss-Messer, M. Schlesinger-Laufer, J. Shainsky-Roitman, A. Schroeder, *J. Controlled Release* **2019**, *296*, 1.
[38] J. Xia, G. Feng, X. Xia, L. Hao, Z. Wang, *Int. J. Nanomed.* **2017**, *12*, 1803.
[39] A. Som, R. Raliya, L. Tian, W. Akers, J. E. Ippolito, S. Singamaneni, P. Biswas, S. Achilefu, *Nanoscale* **2016**, *8*, 12639.
[40] H. Ando, S. E. Emam, Y. Kawaguchi, T. Shimizu, Y. Ishima, K. Eshima, T. Ishida, *Biol. Pharm. Bull.* **2021**, *44*, 844.
[41] I. F. Robey, L. A. Nesbit, *Biomed Res. Int.* **2013**, *2013*, 485196.
[42] S. Harguindey, K. Alfarouk, J. Polo Orozco, S. Fais, J. Devesa, *Int. J. Mol. Sci.* **2020**, *2*, 7475.
[43] S. Pilon-Thomas, K. N. Kodumudi, A. E. El-Kenawi, S. Russell, A. M. Weber, K. Luddy, M. Damaghi, J. W. Wojtkowiak, J. J. Mulé, A. Ibrahim-Hashim, R. J. Gillies, *Cancer Res.* **2016**, *76*, 1381.
[44] V. Huber, C. Camisaschi, A. Berzi, S. Ferro, L. Lugini, T. Triulzi, A. Tuccitto, E. Tagliabue, C. Castelli, L. Rivoltini, *Semin. Cancer Biol.* **2017**, *43*, 74.
[45] C. W. Yun, S. H. Lee, *Int. J. Mol. Sci.* **2018**, *19*, 3466.
[46] J. Lai, B. Chen, H. Mok, G. Zhang, C. Ren, N. Liao, *J. Cell. Mol. Med.* **2020**, *24*, 9145.
[47] K. Jain, K. S. Paranandi, S. Sridharan, A. Basu, *Am. J. Cancer Res.* **2013**, *3*, 251.
[48] C. Ying, C. Jin, S. Zeng, M. Chao, X. Hu, *Oncogene* **2022**, *2022*, 3886.
[49] A. Riemann, M. Rauschner, M. Gießelmann, S. Reime, V. Haupt, O. Thews, *Neoplasia* **2019**, *21*, 450.
[50] C. Stock, M. Mueller, H. Kraehling, S. Mally, J. Noël, C. Eder, A. Schwab, *Cell. Physiol. Biochem.* **2007**, *20*, 679.
[51] R. A. Gatenby, E. T. Gawlinski, *Cancer Res.* **1996**, *56*, 5745.
[52] A. S. Silva, J. A. Yunes, R. J. Gillies, R. A. Gatenby, *Cancer Res.* **2009**, *69*, 2677.
[53] O. Thews, A. Riemann, *Cancer Metastasis Rev.* **2019**, *38*, 113.
[54] M. Bellone, A. Calcinotto, P. Filipazzi, A. De Milito, S. Fais, L. Rivoltini, *Oncoimmunology* **2013**, *2*, 22058.
[55] A. Ibrahim-Hashim, D. Abrahams, P. M. Enriquez-Navas, K. Luddy, R. A. Gatenby, R. J. Gillies, *Cancer Med.* **2017**, *6*, 1720.
[56] A. Ibrahim-Hashim, J. W. Wojtkowiak, M. De, L. C. Ribeiro, V. Estrella, K. M. Bailey, H. H. Cornnell, R. A. Gatenby, R. J. Gillies, *J. Cancer Sci. Ther.* **2011**, *01*, JCST-S1-004.
[57] K. M. Bailey, J. W. Wojtkowiak, H. H. Cornnell, M. C. Ribeiro, Y. Balagurunathan, A. I. Hashim, R. J. Gillies, *Neoplasia* **2014**, *16*, 354.
[58] A. Anemone, L. Consolino, L. Conti, P. Irrera, M. Y. Hsu, D. Villano, W. Dastrù, P. E. Porporato, F. Cavallo, D. L. Longo, *Br. J. Cancer* **2020**, *1241*, 207.
[59] D. Kim, J. H. Lee, H. Moon, M. Seo, H. Han, H. Yoo, H. Seo, J. Lee, S. Hong, P. Kim, H. J. Lee, J. W. Chung, H. Kim, *Theranostics* **2021**, *11*, 79.
[60] D. L. Longo, E. Pirotta, R. Gambino, F. Romdhane, A. Carella, A. Corrado, *Methods Mol. Biol.* **2023**, *2614*, 287.